Size of TiO2 nanoparticles influences their phototoxicity : an in vitro investigation

Xiong, Sijing; George, Saji; Ji, Zhaoxia; Lin, Sijie; Yu, Haiyang; Damoiseaux, Robert; France, Bryan; Ng, Kee Woei; Loo, Say Chye Joachim

2012

Xiong, S., George, S., Ji, Z., Lin, S., Yu, H., Damoiseaux, R., et al. (2012). Size of TiO2 nanoparticles influences their phototoxicity : an in vitro investigation. Archives of toxicology, 87(1), 99-109.

https://hdl.handle.net/10356/99799

https://doi.org/10.1007/s00204-012-0912-5

Size of TiO_2 nanoparticles influences their phototoxicity: an *in vitro* investigation

Sijing Xiong[1], Saji George[2], Zhaoxia Ji[2], Sijie Lin[2], Haiyang Yu[1], Robert Damoiseaux[2], Bryan France[2], Kee Woei Ng[1] and Say Chye Joachim Loo[1*]

1. School of Materials Science & Engineering, Nanyang Technological University, Block N4.1, 50 Nanyang Avenue, Singapore.
2. California NanoSystems Institute, University of California, Los Angeles, California, United States.

[*]Corresponding author: Dr. Joachim Say-Chye Loo, Tel: +65-6790-4603, Fax: +65-6790-9081, Email: JoachimLoo@ntu.edu.sg.

Abstract:

To uncover the size influence of TiO_2 nanoparticles on their potential toxicity, the cytotoxicity of different-sized TiO_2 nanoparticles with and without photoactivation was tested. It was demonstrated that without photoactivation, TiO_2 nanoparticles were inert up to 100 μg/ml. On the contrary, with photoactivation, the toxicity of TiO_2 nanoparticles significantly increased, which correlated well with the specific surface area of the particles. Our results also suggest that the generation of hydroxyl radicals and reactive oxygen species (ROS) mediated damage to the surface adsorbed biomolecules could be the two major reasons for the cytotoxicity of TiO_2 nanoparticles after photoactivation. Higher ROS generation from smaller particles was detected under both biotic and abiotic conditions. Smaller particles could adsorb more proteins, which was confirmed by thermogravimetric analysis. To further investigate the influence of the generation of hydroxyl radicals and adsorption of protein, poly (ethylene-*alt*-maleic anhydride) (PEMA) and chitosan were used to coat TiO_2 nanoparticles. The results confirmed that surface coating of TiO_2 nanoparticles could reduce such toxicity after photoactivation, by hindering adsorption of biomolecules and generation of hydroxyl radical (•OH) during photoactivation.

Key words: titanium dioxide nanoparticles, phototoxicity, cytotoxicity, nanotoxicity, surface coating

1. Introduction

Nanomaterials possess unique properties, arising from their minute sizes, large surface areas and high surface reactivity, and have thus been explored for a wide range of applications such as in sporting goods, cosmetics and electronics (Maynard *et al.* 2006; Xia *et al.* 2006; Nel *et al.* 2006). It was estimated that there are at least 1,300 commercially available products that contain nanomaterials (McCall 2011). Because of this, direct or indirect human contact with nanomaterials becomes inevitable, ultimately raising issues pertaining to their safety (Oberdörster *et al.* 2005; Nel *et al.* 2006; Morris *et al.* 2011; Meng *et al.* 2009). For example, zinc oxide (ZnO) and titanium dioxide (TiO_2) nanoparticles are known active components in most sunscreens. Studies have therefore focused on their cytotoxicity and safety, of which there are studies reporting that ZnO nanoparticles can cause cytotoxicity, resulting from the generation of ROS, mitochondrial depolarization and intracellular calcium ion disturbance (Ng *et al.* 2011; George *et al.* 2009; Heng *et al.* 2010b; Heng *et al.* 2010a). ZnO nanoparticles have also been shown to induce genotoxicity, which have been reported to be likely due to the release of Zn^{2+} ions (George *et al.* 2009; Ng *et al.* 2011).

TiO_2, which is considered as non-soluble, is widely used in the form of nanoparticles across industrial and consumer goods, including cosmetics, paints and food additives, mainly due to their ability to confer opacity and whiteness in different applications (Skocaj *et al.* 2011; Araujo and Nel 2009). In contrast to ZnO, TiO_2 was classified as a biologically inert material, as reported in some studies (Lindenschmidt *et al.* 1990; Ophus *et al.* 1979). TiO_2 was even considered as a “natural” material and is generally positively accepted by the public (Skocaj *et al.* 2011). However, since 1985 it has been shown that photo-activated TiO_2 nanoparticles do

possess antimicrobial properties (Skocaj *et al.* 2011). TiO_2 (anatase) can be excited by light with wavelength shorter than 385 nm (Maness *et al.* 1999). The photons, with sufficient energy, can excite the electrons from the valence band to conduction band, thus generating electron-hole pairs, which will actively react with adsorbed water or oxygen to produce cell-damaging ROS (Bar-Ilan *et al.* 2011; Hoffmann *et al.* 1995). ROS generation is detrimental to many species such as fish and its role in many pathological conditions in human beings is also well documented. Reeves *et al.* (Reeves *et al.* 2008) observed increased damage in TiO_2 treated fish cells after UVA activations, whereby the hydroxyl radicals generated (extracellular and intracellular) were likely responsible for this damage. Nakagawa *et al.* (1997) also pointed out the potential photogenotoxicity of TiO_2 nanoparticles to Chinese hamster cell line. In another study, Gopalan *et al.* (2009) reported that TiO_2 tend to introduce dose-dependent photogenotoxic effect to human lymphocytes but not to human sperms.

However, how particle properties such as size, shape and crystal structure could influence the potential phototoxicity of TiO_2 nanoparticles has not been sufficiently investigated and the possible mechanism has not been fully understood. Jang *et al.*(2001) observed an inverse relationship between TiO_2 particle size and antimicrobial effect after photoactivation, but did not provide the probable mechanism behind this phenomenon. By understanding how a nanomaterial property has an influence on biological activity will provide us an insight on the possible mechanisms behind the toxicity of nanoparticles, and with this understanding find ways to modify their properties and design safer nanomaterials.

In this study, we tested the cytotoxicity of different-sized TiO_2 nanoparticles with and without photo-activation. The particles were photoactivated with UV and near-Vis light, ranging from 280 nm to 450 nm, for 5 min. The short irradiation time was chosen to minimize the toxicity due to light inhibition. Characterization of the nanoparticles, cell viability, generation of ROS and mitochondrial depolarization were conducted to understand the relationship between the nanoparticle properties and their related toxicities. A potential method to decrease such phototoxicity of TiO_2 nanoparticles was also proposed and examined.

2. Materials and Methods

2.1 Preparation of nanoparticles

TiO_2 nanoparticles with primary particles size of 10 nm (T10), 20 nm (T20) and 100 nm (T100) were purchased from SkySpring Nanomaterials Inc., Evonik Industries and MKnano Inc. respectively. All PEMA-coated TiO_2 (T20-PEMA) and chitosan-coated TiO_2 (T20-chitosan) nanoparticles were synthesized in house. PEMA and chitosan were purchased from Sigma and Sinopharm Chemical Reagent Co. Ltd, respectively. In brief, 200 mg TiO_2 nanoparticles (T20) were dispersed in 20 ml of methanol with ultrasonication in an ultrasonic cleaner (MRC laboratory instruments Inc., Holon, Israel) for 30 min. The TiO_2 nanoparticles suspension was added into 18 ml of 0.1% PEMA or chitosan in water. After magnetically stirring for 24 h to evaporate the methanol and allow the coating of PEMA and chitosan on T20 nanoparticles, the samples were freeze dried for 48 h.

2.2 Characterization of TiO_2 nanoparticles

2.2.1 Transmission electron microscopy (TEM)

The primary size of TiO_2 nanoparticles was characterized with Transmission Electron Microscope (TEM, JOEL 2010, Japan). The TiO_2 nanoparticles were first dispersed in methanol and ultrasonicated for 30 min. The dispersed nanoparticles were dropped onto a carbon coated copper grids, and observed under TEM at an accelerating voltage of 200 kV.

2.2.2 Hydrodynamic size and surface charge of particles

The hydrodynamic size and surface charge of the particles were characterized using dynamic light scattering (DLS) technique. The nanoparticles in powder form were dispersed into stock suspension (3 mg/ml) in water or cell culture medium. The stock solution was ultrasonicated for 10 min and then further diluted in water and cell culture medium at a concentration of 30 μg/ml. Further ultrasonication was conducted for another 10 min just before carrying out DLS measurement using a ZetaPALS zeta potential analyzer (Brookhaven instruments, USA).

2.2.3 Theoretical surface area and Brunauer-Emmett-Teller (BET) surface area

The theoretical surface area of TiO_2 nanoparticles was calculated through the true density and diameter of the nanoparticles as from equation (1) (Jang *et al.* 2001).

$$S = {}^{6}/_{\rho d} \qquad \text{Equation (1)}$$

Where S represented the theoretical surface area, ρ was the true density of materials, d was the mean diameter of nanoparticles. The true density of TiO_2 was estimated to be 3.90 g/cm^3 (Tanaka and Suganuma 2001) according to information obtained from the suppliers.

The Brunauer-Emmett-Teller (BET) surface area was tested using micromeritics surface area analyzer (ASAP 2000, USA). The powder of TiO_2 nanoparticles was degassed at 200 °C in flowing nitrogen for 4 h prior to nitrogen adsorption.

2.3 *In vitro* cytotoxicity study

2.3.1 Cell culture

The immortalized mouse macrophage cell line RAW264.7 (ATCC # TIB-71) cells were cultured in cell culture medium which is composed of 88% Dulbecco's Modified Eagle Medium (DMEM) (Gibco), 10% fetal bovine serum (FBS) (Benchmark), 1% sodium pyruvate (Hyclone) and 1% penicilin-streptomycin (Hyclone). The cells were incubated in a humidified atmosphere containing 5% CO_2 at 37 °C and sub-cultured every two days until they reached 70-80% confluence.

2.3.2 Dispersion of TiO_2 nanoparticles

The nanoparticles in powder form were dispersed in cell culture medium into stock suspension (3 mg/ml). This stock suspension was ultrasonicated in water bath for 10 min. The stock suspension was further diluted into a working suspension (100 μg/ml), which was ultrasonicated for another 10 min before adding into cells.

2.3.3 Treatment of nanoparticles with/without photoactivation

RAW264.7 cells at concentration of 20,000 cells / cm^2 were plated in 384-well black plate with transparent bottom, and were allowed to grow for 24 h at 37 °C with 5% CO_2 in a humidified atmosphere. The working suspension of dispersed nanoparticles were added into each well and incubated with cells for another 24 h. For the test groups with UV-Vis exposure, the excess nanoparticles that did not enter or attach onto cells were washed away with 40 μl of PBS using a plate washer, for three times at 21 h. After the wash, cells in each well with 25 μl of PBS were

placed under a 100W xenon arc lamp (LAX-cute, Asahi Spectra) with a light filter to transmit light in the wavelength between 280 nm and 450 nm. The cells were then exposed to UV-Vis light for 5 min. Finally, another 25 μl of cell culture medium was added into each well followed by 3 h incubation in standard cell culture conditions.

2.3.4 Cellular response characterization

Cytotoxicity parameters including plasma membrane damage, mitochondrial superoxide generation and mitochondrial depolarization were recorded utilizing high throughput screening method (George *et al.* 2009). Propidium iodide (PI) nucleic acid stain (Invitrogen, P3566) was utilized to probe the integrity of cell membrane. MitoSOX (Invitrogen, M36008) was used to detect the generation of superoxide in mitochondria. JC-1 (Invitrogen, T3168) could probe the decrease of mitochondrial membrane potential. Hoechst (Invitrogen, H3570) was a membrane permeable dye which could bind on the nucleic acid to indicate the location and total number of both live and dead cells. The cells were washed twice with PBS before adding in 25 μl dye cocktail (Table 1) to incubate for 30 min in the absence of light in standard 37 °C incubator. The fluorescent images were taken by an automated epifluorescence microscope, Image-Xpress^{micro} (Molecular Devices, Sunnyvale, USA) under 10 × magnifications. The percentage of cells showing positive signals was automatically calculated using Meta-Xpress software.

2.4 Abiotic hydroxyl radical generation test

Hydroxyphenyl fluorescein (HPF, H36004) was utilized in this study to probe the hydroxyl radical generation from the TiO_2 nanoparticles under UV-Vis exposure. HPF working solution (100 μM, 5 μl/well) was added into 384-well plate with nanoparticles suspension (100 μg/ml, 45

μl/well) in DI water. The fluorescent intensity (F_0) was tested immediately at Excitation / Emission wavelength of 490 nm / 515 nm using SpectraMax M5e Multi-Mode Microplate Reader (Molecular Devices Corp., USA). After UV-Vis exposure (280 nm-450 nm) for 5 min, the fluorescent intensity (F_1) in each well was tested again. The rate increase of fluorescent intensity per minute was calculated through equation (2).

$$\text{Rate increase of fluorescent intensity (/min)} = (F_1 - F_0)/5 \text{ min} \qquad \text{Equation (2)}$$

2.5 Protein adsorption study

TiO_2 nanoparticles was dispersed in DMEM solution with bovine serum albumin (BSA) at a concentration of 2 mg/ml. T20-PEMA and T20-chitosan was washed three times with DI water beforehand to remove unbound PEMA and chitosan. The particles (1 mg/ml) were ultrasonicated for 20 min in BSA-DMEM solution. All of the particles were collected by centrifugation at 14,000 rpm for 20 min at 25 °C, and washed with DI water for 3 time before freeze-drying for 48 h. Thermo Gravimetric Analyzer (TGA, 2950, HR, V5.4A) was used to test the BSA attached on different particles at a heating rate of 20 °C /min in an nitrogen atmosphere.

2.6 Statistics

All quantitative data are shown as means ± standard deviation. One-way analysis of variance (ANOVA) and Tukey's pairwise comparisons was utilized for multiple comparisons. Significant difference was considered when $p<0.05$. All tests were carried out four times.

3. Results

3.1 Characterization of nanoparticles

TiO_2 nanoparticles of three different sizes were found to be near-spherical in shape as shown from TEM images (Figure 1). The primary particle sizes were 10 nm (T10), 20 nm (T20) and 100 nm (T100). The hydrodynamic size, polydispersity index (PDI) and zeta potential of the nanoparticles were tested through DLS in both DI water and cell culture medium. The results were summarized in Table 2. All the particles showed size in DI water and cell culture medium in the range from 200 to 700 nm. Although different particles exhibited different surface charge in DI water, the zeta potentials in cell culture medium were similar and lie in the range from -5 mV to -10 mV. This could be due to the surface binding of proteins from cell culture medium, rendering them to have similar zeta potential values. All of the three particles are mainly composed of anatase except T20 particles, which contain 19% rutile. The BET surface area measurements showed that the smaller particles had larger specific surface area. The BET surface areas were found to be similar to the theoretically calculated surface areas (from equation (1)) which were calculated based on the size of different particles and the true density of the materials. This result confirmed the primary size of TiO_2 nanoparticles measured from TEM analysis.

3.2 The phototoxicity of TiO_2 nanoparticles was size and surface area dependent.

In this study, RAW264.7 macrophages were used as a model biological system for testing of the phototoxicity of TiO_2 nanoparticles. RAW264.7 cells have been widely utilized in nanotoxicology studies as a model mammalian cell line (RAW 264.7) to understand the cytotoxicity and phototoxicity of TiO_2 nanoparticles (George *et al.* 2011a; Xia *et al.* 2006; Xia *et*

al. 2008). To have a better comparison with other studies, we chose RAW264.7 cells to elucidate the phototoxicity of different sized TiO_2 nanoparticles. The negative control (NC) received neither particles nor UV-Vis light, while light control (LC) received UV-Vis light only. From figure 2, LC showed some damage to cells when compared with NC, but is not statistically significant ($p > 0.05$). This meant that the RAW264.7 cells exposed to UV-Vis light (280-450 nm) for 5 min did not cause any significant cytotoxicity. For the cells treated with non-photoactivated nanoparticles only, the cytotoxicity of the nanoparticles alone is not significant, which is less than 1% for the percentage of positive cells in PI uptake and MitoSOX tests. A slight increase of JC-1 signals (2.5%) was observed in the T10-treated (smallest size) group. However, after photoactivation, all particle-treated cells exhibited obvious increase in PI uptake, which is indicative of cell death. The mortality of T10-treated RAW264.7 cells increased to ~30% after photoactivation, which was significantly higher than the mortality of cells treated with larger particles T20 (9.5%) and T100 (9.0%) with photoactivation. A similar trend in mitochondrial superoxide was also observed to increase, revealing the possible underlying mechanism of cell death – due to generation of reactive oxygen species (ROS) and subsequent induction of oxidative stress in cells. From figure 2, it is evident that T10-treated cells, with photoactivation, showed a higher generation of mitochondrial superoxide when compared to the larger particles of T20 and T100. The JC-1 test revealed a slight decrease in mitochondrial membrane potential compared with non-activated groups. This meant that mitochondrial depolarization could be one of the damages caused by the phototoxicity of TiO_2 nanoparticles but it may not be the main reason responsible for the death of cells.

An inverse relationship between phototoxicity and the size of TiO_2 nanoparticles was observed. This was consistent with the fact that smaller particles had larger surface area per unit mass compared to larger particles. Thus we hypothesized that the higher cytotoxicity induced by smaller particles is related to their higher surface area and thus a larger number of surface-exposed TiO_2 molecules. Particle concentration was then converted from weight/ml into surface area/ml, which was 166.0 cm^2/ml, 50.4 cm^2/ml and 17.2 cm^2/ml for T10, T20 and T100, respectively. From figure 3, the cytotoxicity results showed excellent correlation with the surface area, because the R^2 for PI uptake, MitoSOX and JC-1 results were 0.967, 0.917 and 0.966, respectively. These observations indicated that cell membrane damage, ROS generation and mitochondrial depolarization caused by photoactivated TiO_2 nanoparticles were proportional to the surface area of nanoparticles.

3.3 Surface coating of TiO_2 nanoparticles with PEMA or chitosan decreased phototoxicity.

Since it was shown that phototoxicity was correlated to exposed surface area, it was further hypothesized that the toxic effects would be minimized *via* coating the surface of TiO_2 nanoparticles. To eliminate the influence of surface charge, we chose two differently charged materials to coat the TiO_2 nanoparticles (T20), which are negatively-charged PEMA and positively-charged chitosan. After surface coating with PEMA or chitosan, the Zeta potential of T20 nanoparticles changed from 32.3 mV to -50.4 mV and 51.4 mV respectively (Table 2), showing the successful coating of PEMA or chitosan onto the surface of T20 nanoparticles. From PI uptake results shown in figure 4a, the mortality of photoactivated coated-T20 nanoparticles decreased significantly ($p<0.05$). Similarly, MitoSOX staining results showed that cells with mitochondrial peroxide generation also decreased in both T20-PEMA and T20-

chitosan treated groups compared with T20 nanoparticles treated groups (Figure 4b). Decreased mitochondrial damage was also observed in JC-1 results (Figure 4c). In summary, the surface coating of TiO_2 nanoparticles, regardless of the charge of materials, could decrease the cytotoxicity of TiO_2 nanoparticles during photoactivation.

3.4 Hydroxyl radical generation was responsible for the phototoxicity of TiO_2 nanoparticles.

Based on figure 5, smaller particles tend to have a higher rate of hydroxyl radical generation under photoactivation in abiotic conditions. This could be due to two reasons. First, for smaller particles, more photoactivated electrons and holes could reach the TiO_2 surfaces. Second, more molecules such as H_2O and O_2 are adsorbed onto TiO_2 surfaces to interact with these photoactivated electrons and holes to generate more hydroxyl radicals (Zhang *et al.* 2010). Surface coating of T20 nanoparticles with PEMA or chitosan was shown to significantly decreased the generation of hydroxyl radicals ($p<0.05$).

3.5 Protein adsorption was size dependent and decreased after surface coating of TiO_2 nanoparticles.

It was shown that smaller particles tended to generate more hydroxyl radicals during photoactivation. The hydroxyl radicals are viciously reactive, which attacks whatever nearby and reacts at the site of formation (Vidosava B 2004; Halliwell 1996). Intuitively, if smaller particles could adsorb more biomolecules onto their surface, this would increase the possibility that these biomolecules could be damaged by photo-activated hydroxyl radicals. BSA was therefore chosen as a model to understand the adsorption ability of biomolecules onto different sized nanoparticles. BSA is a type of biomolecules which will gradually decompose with the increase of temperature;

however, TiO_2 nanoparticles are relatively stable with temperature below 600 °C. So TGA analysis technique can be utilized to semi-quantify the amount the BSA attached onto TiO_2 nanoparticles (Simi and Abraham 2009). Figure 6 shows the TGA analysis of pure BSA, nanoparticles and nanoparticles-BSA. From figure 6a, a major weight loss of BSA protein was observed from 188 °C to 485 °C, corresponding to its decomposition temperature. Based on figure 6b, T10-BSA, T20-BSA and T100-BSA nanoparticles exhibited a much larger mass loss within this temperature range compared to their uncoated counterparts T10, T20 and T100 nanoparticles, corresponding to mass loss due to the adsorbed BSA. It was also shown that smaller particles (T10 and T20) adsorbed more BSA than larger particles (T100). From figure 6c, the T20-PEMA and T20-chitosan particles also showed a mass loss, which proved the successful surface coating of PEMA and chitosan onto T20 nanoparticles. Although there are mass loss observed for T20-PEMA and T20-chitosan nanoparticles, T20-PEMA, T20 and T20-chitosan nanoparticles still exhibited lower drop in mass at the decomposition temperature range of BSA as compared to counterpart T20-PEMA-BSA, T20-BSA and T20-chitosan-BSA nanoparticles. The difference in weight loss between BSA adsorbed nanoparticles and corresponding nanoparticles indicated the amount of BSA attached on the particles, which was in the following sequences T20>T20-chitosan>T20-PEMA. This result confirms that surface coating of T20 nanoparticles with PEMA or chitosan could decrease the BSA adsorption on T20 nanoparticles.

4. Discussion

The hypothesis of this study was that phototoxicity of TiO_2 nanoparticles was size dependent. We chose TiO_2 nanoparticles of different sizes to conduct this study. T20 is the most widely used and studied Degussa TiO_2 P25 nanoparticles, which composed of 81% anatase and 19% rutile (Ji

et al. 2010). To understand the mechanism behind the phototoxicity of this particle can provide valuable information in the application of Degussa P25 nanoparticles. To study the size effect on the phototoxicity of TiO_2 nanoparticles, we chose another two particles T10 and T100, which composed of anatase. X-ray powder diffraction (XRD) patterns of T10, T20 and T100 nanoparticles were shown in supporting information figure S1, which indicated the crystal structure of these three TiO_2 nanoparticles. RAW264.7 cells were treated with TiO_2 nanoparticles of different sizes with and without UV-Vis excitation. The PI staining test exhibited that the lethal toxicity of TiO_2 nanoparticles after UV-Vis activation was size-dependent. Smaller particles, with correspondingly larger surface area, tend to cause higher cytotoxicity as compared to larger particles (smaller surface area) of the same concentration. To uncover the mechanism behind the phototoxic effect of TiO_2 nanoparticles, a multi-parametric cytotoxicity analysis was carried out. The intracellular perturbations included mitochondrial superoxide generation and mitochondrial depolarization. Based on figure 3, the mitochondrial superoxide production, mitochondrial depolarization and loss of cell plasma membrane integrity correlated well with the specific surface area of the particles (R^2>0.9). To understand the cause of oxidative stress in cells, we tested the generation of hydroxyl radicals during photoactivation of TiO_2 nanoparticles in an abiotic condition. The results of HPF test point out that oxidative stress in cells could be due to the ROS generated by photoactivated TiO_2 nanoparticles directly.

With our results, we present here a model to describe the potential mechanism of TiO_2 nanoparticles induced phototoxicity, as shown in figure 7. When TiO_2 nanoparticles are exposed to UV light, the photon energy excites the electrons (e^-) in the valence band to the conduction band and leave holes (h^+) in the valence band, giving rise to electron hole pairs (Maness *et al.*

1999). The holes (h^+) can interact with adsorbed H_2O or hydroxide ions (OH^-) to generate hydroxyl radicals (•OH) which are highly reactive and damaging to cells (Dröge 2002), as hydroxyl radicals (•OH) can inflict detrimental damage on cellular proteins, lipids and even DNA, resulting in the oxidation and dysfunction of biomolecules (Maness *et al.* 1999; Almquist and Biswas 2002; George *et al.* 2011b; Circu and Aw 2010; Finkel and Holbrook 2000). Furthermore, the electrons (e^-) in the conduction band can reduce oxygen (O_2) adsorbed onto the particle surface to produce superoxide ions (O_2^-), which can further react with water in the environment to form hydrogen peroxide in cells (Brookes *et al.* 2004; George *et al.* 2011a). ROS generation is widely considered as a molecular paradigm for the toxicity of nanoparticles (Xia *et al.* 2006). Excessive ROS generation would cause oxidative stress in cells (Perraud *et al.* 2004; Tan *et al.* 1998). If the oxidative stress exceeds the threshold of the cellular antioxidant defenses, additional mitochondrial perturbation such as mitochondrial depolarization would occur (Nel *et al.* 2006; Lin and Beal 2006; Brookes *et al.* 2004). These disturbances might further cause apoptosis or necrosis of cells followed by an increase in cell membrane permeability. From the current results, we found that the phototoxicity of TiO_2 nanoparticles to RAW264.7 cells could be mainly due to the ROS generation. ROS could be spontaneously generated by the materials or during the interaction between particles and cellular components (Xia *et al.* 2006). HPF results indicated that ROS generation may result directly from hydroxyl radicals generated by photoactivated TiO_2 nanoparticles.

Furthermore, we found the size dependent cytotoxicity of TiO_2 nanoparticles after photoactivation could be due to two reasons, size dependent ROS generation and size dependent biomolecule adsorption. Smaller particles with higher percentage of molecules on their surface

(Oberdörster *et al.* 2005) can generate more ROS such as •OH, which was proved by HPF test. The highly unstable hydroxyl radicals can non-specifically attack biomolecules such as DNA, proteins and lipids in a diffusion-controlled reaction (Vidosava B 2004). The damage of proteins induced by oxidative stress has been widely studied. The formation of carbonyl derivatives is considered as one of the possible modifications caused by oxidative stress, which is through oxidation-induced peptide cleavage or direct oxidation of certain amino-acid side chains (Finkel and Holbrook 2000; Stadtman 1992). Biomolecules such as proteins attached onto the surface of TiO_2 nanoparticles enhanced the likelihood to be damaged or denatured by the hydroxyl radicals on the surface TiO_2 nanoparticles. Obviously, if this reaction happens to some key biomolecules such as DNA, proteins and lipids, the state of the cells will be affected (Vidosava B, 2004). For example, if the lipid peroxidation happened in cellular membrane, the fluidity of membrane will decrease, resulting in increased permeability for ions (Vidosava B 2004). The oxidized protein would increase the susceptibility to enzymic proteolysis (Dukan *et al.* 2000). Smaller particles with more TiO_2 molecules exposed on the surface of TiO_2 nanoparticles can adsorb more biomolecules such as proteins on their surfaces. The protein adsorption study proved that smaller particles with higher surface area could adsorb more proteins, similarly shown by Horie *et al.* (2009). Thus, more biomolecules tend to be damaged by smaller TiO_2 nanoparticles.

Based on the previous results, we further hypothesized that if the surface of TiO_2 nanoparticles was pre-coated with other materials, the phototoxicity of TiO_2 nanoparticles should decrease. We used PEMA and chitosan to coat T20 nanoparticles. Cytotoxic tests showed obvious decrease in phototoxicity after surface coating of T20 nanoparticles based on PI uptake and MitoSOX staining results. The HPF test further proved that the surface coating of T20 nanoparticles could

decrease hydroxyl radicals (•OH) generation by T20 during the photoactivation process. The decreased cytotoxicity could be due to four possibilities. First, the surface coating decreased the effective surface area for interaction between surface TiO_2 molecules and other molecules such as water and oxygen. The active electron hole pair may recombine and release the energy in the form of heat (Almquist, 2002). Second, the PEMA or chitosan attached on the surface of TiO_2 nanoparticles quenched the activity of photo-activated TiO_2 surface and resulted in non-harmful oxidized PEMA or chitosan, which prevent further disturbance inside cells. Third, the surface coating of TiO_2 nanoparticles may decrease light intensity reached at the particles. Based on the UV-Vis test (supporting information, Figure S2), the absorbance of UV light largely decreased after coating with PEMA, which indicated that these coated particles are less able to absorb UV and thus reduce the possibilities of free radical formation. The fourth reason could be that there is less BSA adsorption for the coated particles. For example, BSA adsorption on T20 nanoparticles decreased after surface coating. From figure 7, PEMA or chitosan on the surface of TiO_2 nanoparticles might be able to block the attachment of biomolecules on the surface of TiO_2 nanoparticles. The decreased adsorption of biomolecules decreased the possibility of biomolecules to be damaged by ROS, and thus cytotoxicity.

This study provided a novel clue to understand the mechanism behind the phototoxicity of different-sized TiO_2 nanoparticles. These findings showed that the surface area and more specifically, the number of TiO_2 molecules exposed on the surface of TiO_2 nanoparticles can be used to predict the potential phototoxic effects of TiO_2 nanoparticles. With this understanding, we can find ways to modify the phototoxicity of TiO_2 nanoparticles and design safer nanomaterials. Despite the increased toxicity shown in smaller TiO_2 nanoparticles, they have the

potential to be used in biomedical applications. It was reported that photoactivated TiO_2 nanoparticles could selectively induce toxicity against cancer cells (Cai *et al.* 1992; Lagopati *et al.* 2010; Stefanou *et al.* 2010). On the other hand, the surfaces of these particles can be coated with materials such as PEMA and chitosan to reduce their potential toxic effects, for use in consumer products such as sunscreens. But the current results are not adequate to conclude whether the size or size related properties such as surface area played a more important role, which will be the focus of future studies. Further studies are also needed to understand the interaction between TiO_2 nanoparticles and biomolecules. These findings have great potential to be used to predict the cytotoxicity and phototoxicity of different TiO_2 nanoparticles in an abiotic condition.

5. Conclusion

In this study, we demonstrated that the TiO_2 nanoparticles exhibited increased cytotoxicity upon UV-Vis activation in a size-dependent manner. The size-related property, active surface area, could be related to such size-dependent phototoxicity of TiO_2 nanoparticles. ROS generation and biomolecule adsorption could be the two major reasons responsible for the increased cytotoxicity of smaller particles after photoactivation. Higher ROS generation from smaller particles was detected under both biotic and abiotic conditions. TGA analysis revealed that more protein could be adsorbed onto smaller nanoparticles. The surface coating of TiO_2 nanoparticles with PEMA or chitosan could decrease their phototoxicity, which might be due to the hindrance of biomolecule adsorption and hydroxyl radicals (•OH) production in the photo-activation process. This provided the mechanism behind the phototoxicity of TiO_2 nanoparticles and clues on how to alleviate such toxicity.

Acknowledgments

The authors would like to acknowledge the financial support from the Agency for Science, Technology and Research (A*STAR) (Project No: 102 129 0098), the National Medical Research Council (NMRC/EDG/0062/2009) and the Nanyang Institute of Technology in Health & Medicine (NITHM), Singapore. Acknowledgements to the Ian Ferguson Postgraduate Fellowship for Sijing Xiong's research attachment at the University of California, Los Angeles (UCLA). We thank Dr. Andre E. Nel and Dr. Tian Xian (UC Center for Environmental Implications of Nanotechnology) for their kind help in enabling this study.

Conflict of interest The authors have declared no conflict of interest.

References

Almquist CB, Biswas P (2002) Role of synthesis method and particle size of nanostructured TiO2 on its photoactivity. Journal of Catalysis 212 (2):145-156

Araujo JA, Nel AE (2009) Particulate matter and atherosclerosis: role of particle size, composition and oxidative stress. Part Fibre Toxicol 6:19. doi:2410.1186/1743-8977- 6-24

Bar-Ilan O, Louis KM, Yang SP, Pedersen JA, Hamers RJ, Peterson RE, Heideman W (2011) Titanium dioxide nanoparticles produce phototoxicity in the developing zebrafish. Nanotoxicology 0 (0):1-10. doi:doi:10.3109/17435390.2011.604438

Brookes PS, Yoon YS, Robotham JL, Anders MW, Sheu SS (2004) Calcium, ATP, and ROS: a mitochondrial love-hate triangle. Am J Physiol-Cell Physiol 287 (4):C817-C833. doi:10.1152/ajpcell.00139.2004

Cai R, Kubota Y, Shuin T, Sakai H, Hashimoto K, Fujishima A (1992) Induction of cytotoxicity by photoexcited TiO2 particles. Cancer Research 52 (8):2346-2348

Circu ML, Aw TY (2010) Reactive oxygen species, cellular redox systems, and apoptosis. Free Radic Biol Med 48 (6):749-762. doi:10.1016/j.freeradbiomed.2009.12.022

Dröge W (2002) Free radicals in the physiological control of cell function. Physiological reviews 82 (1):47-95

Dukan S, Farewell A, Ballesteros M, Taddei F, Radman M, Nystrom T (2000) Protein oxidation in response to increased transcriptional or translational errors. Proc Natl Acad Sci U S A 97 (11):5746-5749. doi:10.1073/pnas.100422497

Finkel T, Holbrook NJ (2000) Oxidants, oxidative stress and the biology of ageing. Nature 408 (6809):239-247

George S, Pokhrel S, Ji Z, Henderson BL, Xia T, Li L, Zink JI, Nel AE, Madler L (2011a) Role of Fe doping in tuning the band gap of TiO2 for the photo-oxidation-induced 20 cytotoxicity paradigm. Journal of the American Chemical Society 133 (29):11270- 11278. doi:10.1021/ja202836s

George S, Pokhrel S, Xia T, Gilbert B, Ji Z, Schowalter M, Rosenauer A, Damoiseaux R, Bradley KA, Madler L, Nel AE (2009) Use of a rapid cytotoxicity screening approach to engineer a safer zinc oxide nanoparticle through iron doping. ACS Nano 4 (1):15-29. doi:10.1021/nn901503q

George S, Xia T, Rallo R, Zhao Y, Ji Z, Lin S, Wang X, Zhang H, France B, Schoenfeld D, Damoiseaux R, Liu R, Lin S, Bradley KA, Cohen Y, Nel AE (2011b) Use of a high-throughput screening approach coupled with in vivo zebrafish embryo screening to develop hazard ranking for engineered nanomaterials. ACS Nano 5 (3):1805-1817. doi:10.1021/nn102734s

Gopalan RC, Osman IF, Amani A, De Matas M, Anderson D (2009) The effect of zinc oxide and titanium dioxide nanoparticles in the Comet assay with UVA photoactivation of human sperm and lymphocytes. Nanotoxicology 3 (1):33-39

Halliwell B (1996) Antioxidants in human health and disease. Annu Rev Nutr 16:33-50. doi:10.1146/annurev.nutr.16.1.33

Heng BC, Zhao X, Xiong S, Ng KW, Boey FY-C, Loo JS-C (2010a) Toxicity of zinc oxide (ZnO) nanoparticles on human bronchial epithelial cells (BEAS-2B) is accentuated by oxidative stress. Food and Chemical Toxicology 48 (6):1762-1766

Heng BC, Zhao X, Xiong S, Ng KW, Boey FYC, Loo JSC (2010b) Cytotoxicity of zinc oxide (ZnO) nanoparticles is influenced by cell density and culture format. Archives of Toxicology 85 (6):695-704. doi:10.1007/s00204-010-0608-7

Hoffmann MR, Martin ST, Choi W, Bahnemann DW (1995) Environmental Applications of Semiconductor Photocatalysis. Chemical Reviews 95 (1):69-96. doi:10.1021/cr00033a004

Horie M, Nishio K, Fujita K, Endoh S, Miyauchi A, Saito Y, Iwahashi H, Yamamoto K, Murayama H, Nakano H, Nanashima N, Niki E, Yoshida Y (2009) Protein adsorption of ultrafine metal oxide and its influence on cytotoxicity toward cultured cells. Chemical Research in Toxicology 22 (3):543-553. doi:10.1021/tx800289z

Jang HD, Kim S-K, Kim S-J (2001) Effect of particle size and phase composition of titanium dioxide nanoparticles on the photocatalytic properties. Journal of Nanoparticle Research 3 (2):141-147. doi:10.1023/a:1017948330363

Ji Z, Jin X, George S, Xia T, Meng H, Wang X, Suarez E, Zhang H, Hoek EMV, Godwin H, Nel AE, Zink JI (2010) Dispersion and Stability Optimization of TiO2 Nanoparticles in Cell Culture Media. Environ Sci Technol 44 (19):7309-7314. doi:10.1021/es100417s

Lagopati N, Kitsiou PV, Kontos AI, Venieratos P, Kotsopoulou E, Kontos AG, Dionysiou DD, Pispas S, Tsilibary EC, Falaras P (2010) Photo-induced treatment of breast epithelial cancer cells using nanostructured titanium dioxide solution. Journal of Photochemistry and Photobiology A: Chemistry 214 (2-3):215-223

Lin MT, Beal MF (2006) Mitochondrial dysfunction and oxidative stress in neurodegenerative diseases. Nature 443 (7113):787-795

Lindenschmidt RC, Driscoll KE, Perkins MA, Higgins JM, Maurer JK, Belfiore KA (1990) The comparison of a fibrogenic and two nonfibrogenic dusts by bronchoalveolar lavage. Toxicology and Applied Pharmacology 102 (2):268-281

Maness PC, Smolinski S, Blake DM, Huang Z, Wolfrum EJ, Jacoby WA (1999) Bactericidal activity of photocatalytic TiO2 reaction: Toward an understanding of its killing mechanism. Appl Environ Microbiol 65 (9):4094-4098

Maynard AD, Aitken RJ, Butz T, Colvin V, Donaldson K, Oberdorster G, Philbert MA, Ryan J, Seaton A, Stone V, Tinkle SS, Tran L, Walker NJ, Warheit DB (2006) Safe handling of nanotechnology. Nature 444 (7117):267-269

McCall MJ (2011) Environmental, health and safety issues Nanoparticles in the real world. Nat Nanotechnol 6 (10):613-614

Meng H, Xia T, George S, Nel AE (2009) A predictive toxicological paradigm for the safety assessment of nanomaterials. ACS Nano 3 (7):1620-1627. doi:10.1021/nn9005973

Morris J, Willis J, De Martinis D, Hansen B, Laursen H, Sintes JR, Kearns P, Gonzalez M (2011) Science policy considerations for responsible nanotechnology decisions. Nat Nano 6 (2):73-77

Nakagawa Y, Wakuri S, Sakamoto K, Tanaka N (1997) The photogenotoxicity of titanium dioxide particles. Mutation Research/Genetic Toxicology and Environmental Mutagenesis 394 (1-3):125-132

Nel A, Xia T, Madler L, Li N (2006) Toxic potential of materials at the nanolevel. Science 311 (5761):622-627. doi:10.1126/science.1114397

Ng KW, Khoo SPK, Heng BC, Setyawati MI, Tan EC, Zhao X, Xiong S, Fang W, Leong DT, Loo JSC (2011) The role of the tumor suppressor p53 pathway in the cellular DNA damage response to zinc oxide nanoparticles. Biomaterials 32 (32):8218-8225

Oberdörster G, Oberdörster E, Oberdörster J (2005) Nanotoxicology: An emerging discipline evolving from studies of ultrafine particles. Environ Health Perspect 113 (7):823-839. doi:10.1289/ehp.7339

Ophus EM, Rode L, Gylseth B, Nicholson DG, Saeed K (1979) Analysis of titanium pigments in human lung tissue Scand J Work Environ Health 5 (3):290-296

Perraud AL, Knowles HM, Schmitz C (2004) Novel aspects of signaling and ion-homeostasis regulation in immunocytes: The TRPM ion channels and their potential role in modulating the immune response. Molecular Immunology 41 (6-7):657-673

Reeves JF, Davies SJ, Dodd NJF, Jha AN (2008) Hydroxyl radicals (OH) are associated with titanium dioxide (TiO2) nanoparticle-induced cytotoxicity and oxidative DNA damage in fish cells. Mutation Research/Fundamental and Molecular Mechanisms of Mutagenesis 640 (1-2):113-122

Simi CK, Abraham TE (2009) Nanocomposite based on modified TiO2-BSA for functional applications. Colloid Surf B-Biointerfaces 71 (2):319-324.doi:10.1016/j.colsurfb.2009.02.019

Skocaj M, Filipic M, Petkovic J, Novak S (2011) Titanium dioxide in our everyday life; is it safe? Radiol Oncol 45 (4):227-247. doi:10.2478/v10019-011-0037-0

Stadtman ER (1992) Protein oxidation and aging. Science 257 (5074):1220-1224. doi:10.1126/science.1355616

Stefanou E, Evangelou A, Falaras P (2010) Effects of UV-irradiated titania nanoparticles on cell proliferation, cancer metastasis and promotion. Catalysis Today 151 (1- 2):58-63

Tan S, Sagara Y, Liu Y, Maher P, Schubert D (1998) The regulation of reactive oxygen species production during programmed cell death. J Cell Biol 141 (6):1423-1432. doi:10.1083/jcb.141.6.1423

Tanaka Y, Suganuma M (2001) Effects of heat treatment on photocatalytic property of sol¬gel derived polycrystalline TiO2. J Sol-Gel Sci Technol 22 (1-2):83-89. doi:10.1023/a:1011268421046

Vidosava B D (2004) Free radicals in cell biology. In: International Review of Cytology, vol Volume 237. Academic Press, Serbia and Montenegro, pp 57-89

Xia T, Kovochich M, Brant J, Hotze M, Sempf J, Oberley T, Sioutas C, Yeh JI, Wiesner MR, Nel AE (2006) Comparison of the abilities of ambient and manufactured nanoparticles to induce cellular toxicity according to an oxidative stress paradigm. Nano Letters 6 (8):1794-1807

Xia T, Kovochich M, Liong M, Mädler L, Gilbert B, Shi H, Yeh JI, Zink JI, Nel AE (2008) Comparison of the mechanism of toxicity of zinc oxide and cerium oxide nanoparticles based on dissolution and oxidative stress properties. ACS Nano 2 (10):2121-2134. doi:10.1021/nn800511k

Xiong S, Zhao X, Heng BC, Ng KW, Loo JSC (2011) Cellular uptake of Poly-(D, L-lactide-co-glycolide) (PLGA) nanoparticles synthesized through solvent emulsion evaporation and nanoprecipitation method. Biotechnol J 6(5):501–508

Zhang JL, Wages M, Cox SB, Maul JD, Li YJ, Barnes M, Hope-Weeks L, Cobb GP (2010) Effect of titanium dioxide nanomaterials and ultraviolet light coexposure on African clawed frogs (Xenopus laevis). Environ Toxicol Chem 31 (1):176-183. doi:10.1002/etc.718

Zhao XX, Heng BC, Xiong SJ, Guo J, Tan TTY, Boey FYC, Ng KW, Loo JSC (2010) In vitro assessment of cellular responses to rodshaped hydroxyapatite nanoparticles of varying lengths and surface areas. Nanotoxicology 5(2):182–194. doi:10.3109/17435 390.2010.503943

Zhao X, Ng S, Heng BC, Guo J, Ma L, Tan TTY, Ng KW, Loo SCJ (2012) Cytotoxicity of hydroxyapatite nanoparticles is shape and cell dependent. Arch Toxicol, 1–16. doi:10.1007/s00204-012-0827-1

Table 1 Three groups of probe cocktails used

Fluorescence probe cocktail	Ex/Em wavelength (nm)	Indication
1 μM Hoechst + 5 μM PI	355/465 & 540/620	Damaged plasma membrane integrity
1 μM Hoechst + 5 μM MitoSOX	355/465 & 510/580	Generation of mitochondrial superoxide
1 μM Hoechst +1 μM JC-1	355/465 & 480/530-590	Mitochondrial depolarization

Table 2 Characterization of TiO_2 nanoparticles with different size and surface coating

		T10	T20	T100	T20-PEMA	T20-chitosan
Primary Particle Size (nm)		10	20	100	20	20
Cristal structure		Anatase	Ana*/Rut* 81/19	Anatase	/	/
water	Size (nm)	669	307	349	643	408
	PDI	0.186	0.263	0.224	0.349	0.276
	Zeta Potential (mV)	-16.9	32.3	19.1	-50.4	51.4
CDMEM	Size (nm)	262	338	444	633	742
	PDI	0.005	0.180	0.248	0.330	0.306
	Zeta Potential (mV)	-5.7	-7.7	-9.3	-9.6	-7.2
Theoretical Surface Area (m^2/g)		154	73	15	/	/
BET Surface Area (m^2/g)		166.0	50.4	17.2	/	/

Ana* represents anatase
Rut* represents rutile

Fig.1 TEM micrographs of 3 spherical TiO_2 nanoparticle samples with different sizes. (a) T10, 10nm; scale bar 20 nm, (b) T20, 20nm; scale bar 20 nm, (c) T100, 100nm; scale bar 100 nm

Fig.2 Potential damage to RAW264.7 cells after being treated with or without UV light (280 nm - 450 nm) for 5 min. NC represented negative control which received neither particles nor UV light. LC represented light control which received UV light only. For test groups (T10, T20 and T100), the cells were treated with the different nanoparticles at 100 μg/ml. Cells were stained with (a) PI, (b) MitoSOX and (c) JC-1 to probe cytoplasm membrane integrity, mitochondrial superoxide generation and mitochondrial depolarization, respectively. Smaller particles triggered higher levels of phototoxicity to cells in all 3 assays. Data represents means ± SD, n=4. * $p<0.05$ compared with corresponding control (NC is control for non UV exposed group; LC is control for UV exposed group.). # $p<0.05$ compared with other two particles treated groups

Fig.3 Toxicity of photoactivated TiO_2 nanoparticles was correlated with surface area. The surface areas normalized to volume were 166.0 cm^2/ml, 50.4 cm^2/ml and 17.2 cm^2/ml for T10, T20 and T100, respectively. Cytotoxicity outcome showed excellent correlation with the surface area for (a) PI uptake, (b) MitoSOX and (c) JC-1 results ($R^2>0.9$). Data represents means ± SD, n=4

Fig.4 Potential damage to RAW264.7 cells after being treated with or without UV light exposure (280 nm - 450 nm) for 5 min. NC represented negative control which received neither particles nor UV light. LC represented light control which received UV light only. For test groups (T20-PEMA, T20 and T20-chitosan), the cells were treated with different nanoparticles at a

concentration of 100 μg/ml, and assayed for (a) PI uptake, (b) MitoSOX staining and (c) JC-1 staining. After surface coating with PEMA or chitosan, the phototoxicity of T20 nanoparticles decreased. Data represents means ± SD, n=4. * p<0.05 compared with corresponding control (NC is control for non UV exposed group; LC is control for UV exposed group.). # p<0.05 compared with the other particles treated group

Fig.5 Hydroxyl radical genenation during photoactivation of TiO_2 nanoparticles tested by HPF assay. Smaller particles generated more hydroxyl radicals during photoactivation of TiO_2 nanoparticles. The surface coating of T20 nanoparticles with PEMA or chitosan significantly decreased the hydroxyl radicals generated by T20 nanoparticles. Data represents means ± SD, n=4. * p<0.05 between T10, T20 and T100. # p<0.05 between T20-PEMA, T20 and T20-chitosan

Fig.6 TGA analysis of BSA adsorption onto TiO_2 nanoparticles. (a) BSA, (b) T10, T20, T100 and their corresponding BSA adsorbed nanoparticles, (c) T20, T20-PEMA, T20-chitosan and their corresponding BSA adsorbed nanoparticles. Smaller particles absorbed more BSA than bigger particles. The surface coating of T20 nanoparticles with PEMA or chitosan decreased the BSA adsorption onto T20 nanoparticles.

Fig.7 Schematic of the possible mechanism behind the phototoxicity of TiO_2 nanoparticles. When TiO_2 nanoparticles are exposed to UV light, the photon energy excite the electrons (e^-) in the valence band to the conduction band and leave holes (h^+) in the valence band to form electron hole pairs. The holes (h^+) can interact with adsorbed H_2O or hydroxide ions (OH^-) to generate

reactive hydroxyl radicals (•OH) which can interact with biomolecules nearby and result in the oxidation and dysfunction of biomolecules. The electrons (e^-) in the conduction band can reduce oxygen (O_2) adsorbed onto the particle surface to produce superoxide ions (O_2^-), which can further react with water in the environment to form hydrogen peroxide in cells. Surface coating of TiO_2 nanoparticles with PEMA or chitosan can effectively decrease generation of hydroxyl radicals (•OH) and adsorption of biomolecules.

Figure 1

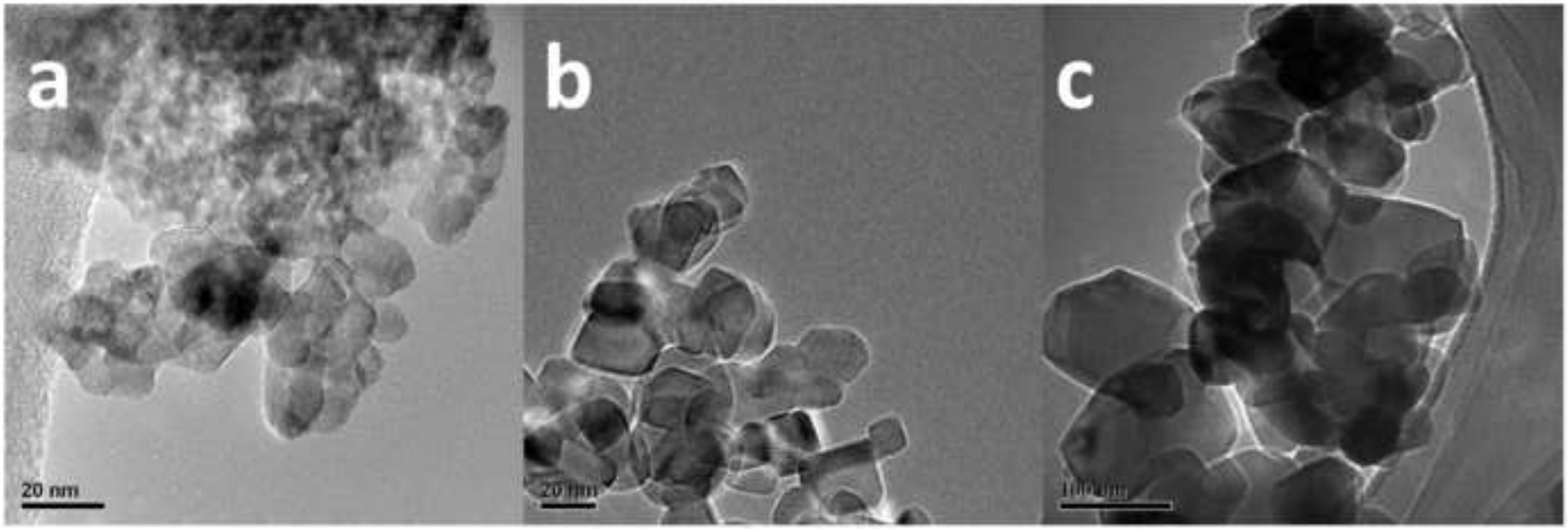

Figure 2

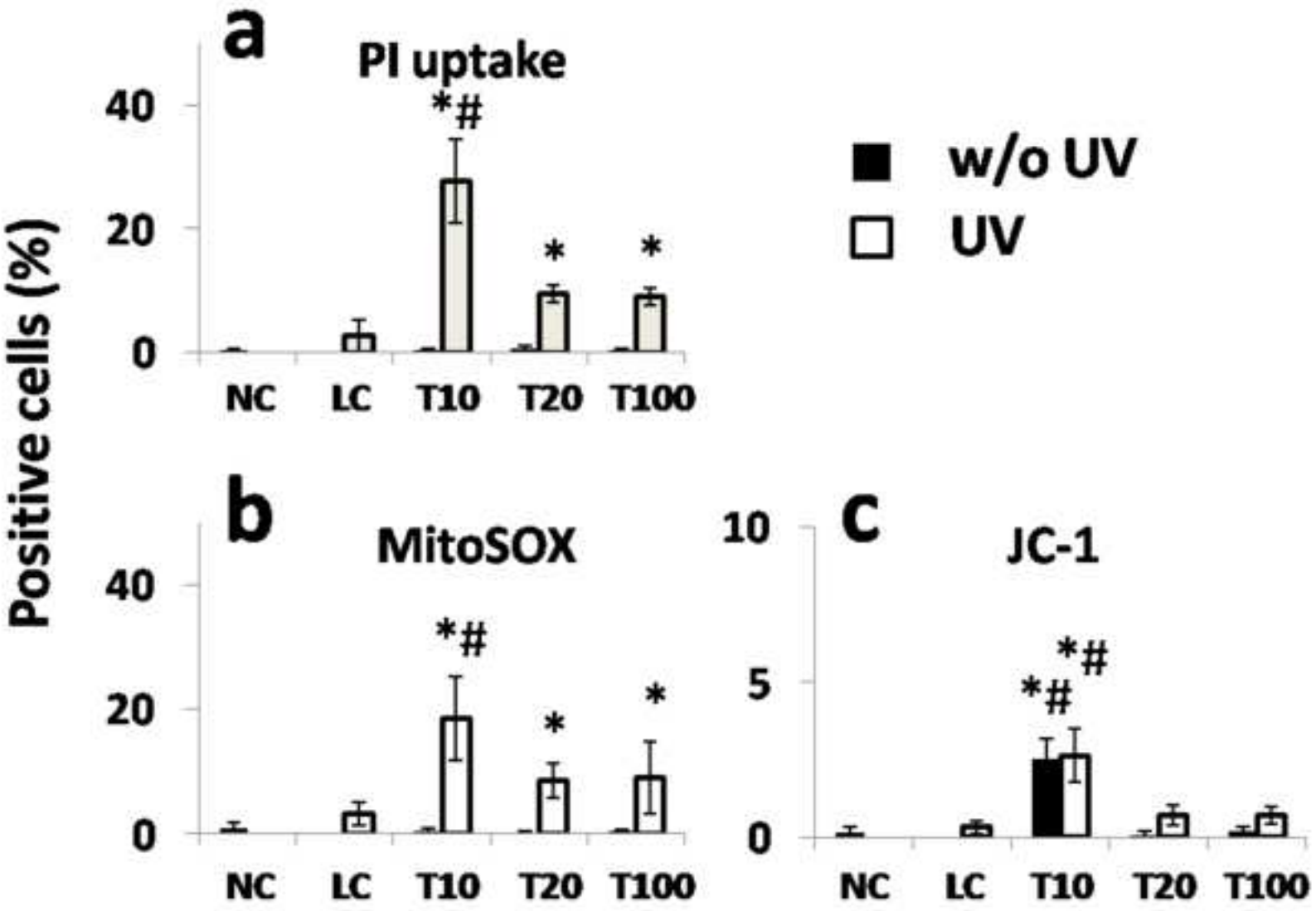
a
PI uptake
b
MitoSOX
c
JC-1
Positive cells (%)
w/o UV
UV
NC
LC
T10
T20
T100
0
20
40
5
10
*
#

Figure 3

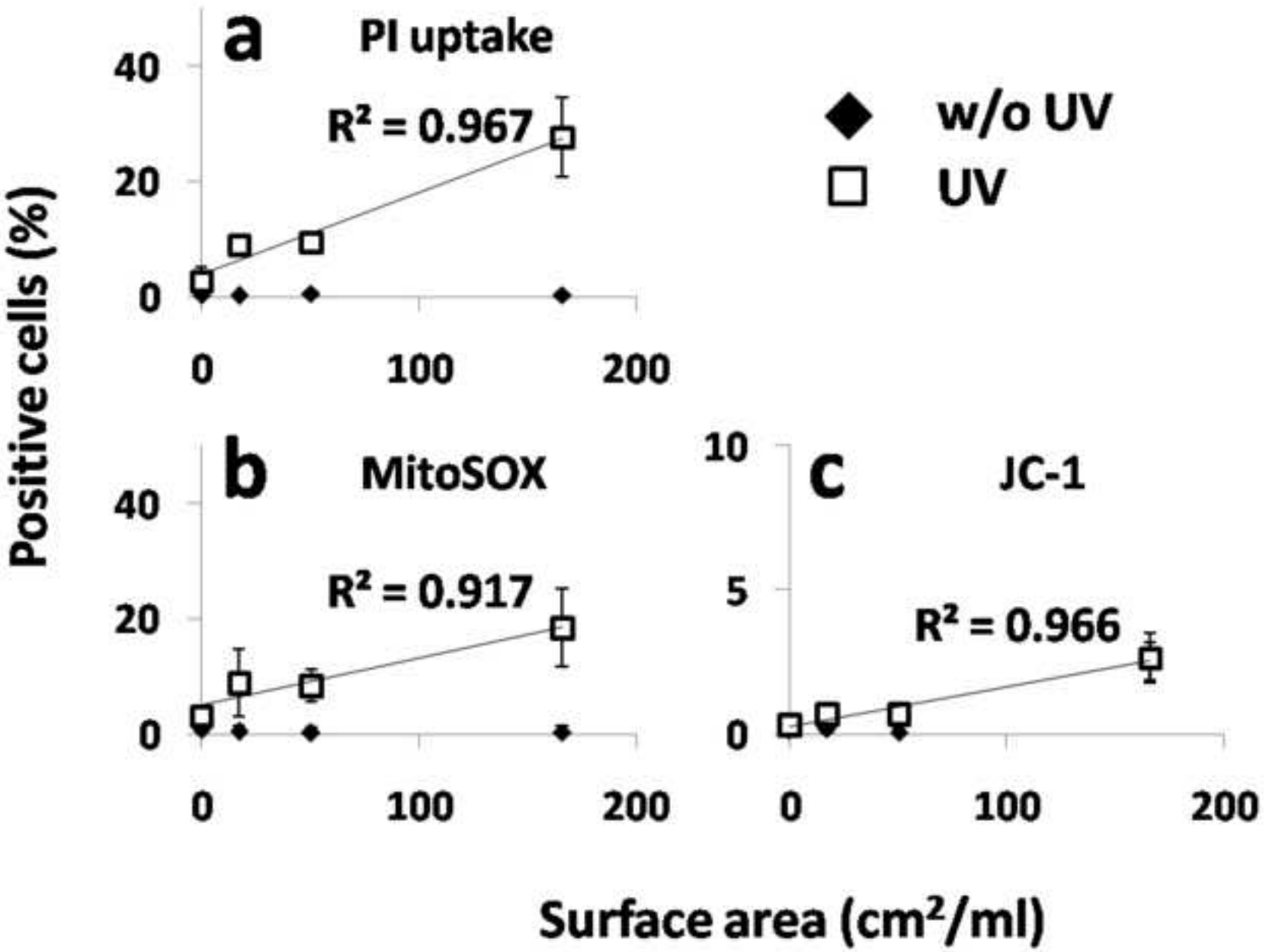
a
PI uptake
R² = 0.967
w/o UV
UV
Positive cells (%)
40
20
0
0
100
200
b
MitoSOX
R² = 0.917
40
20
0
0
100
200
c
JC-1
R² = 0.966
10
5
0
0
100
200
Surface area (cm²/ml)

Figure 4

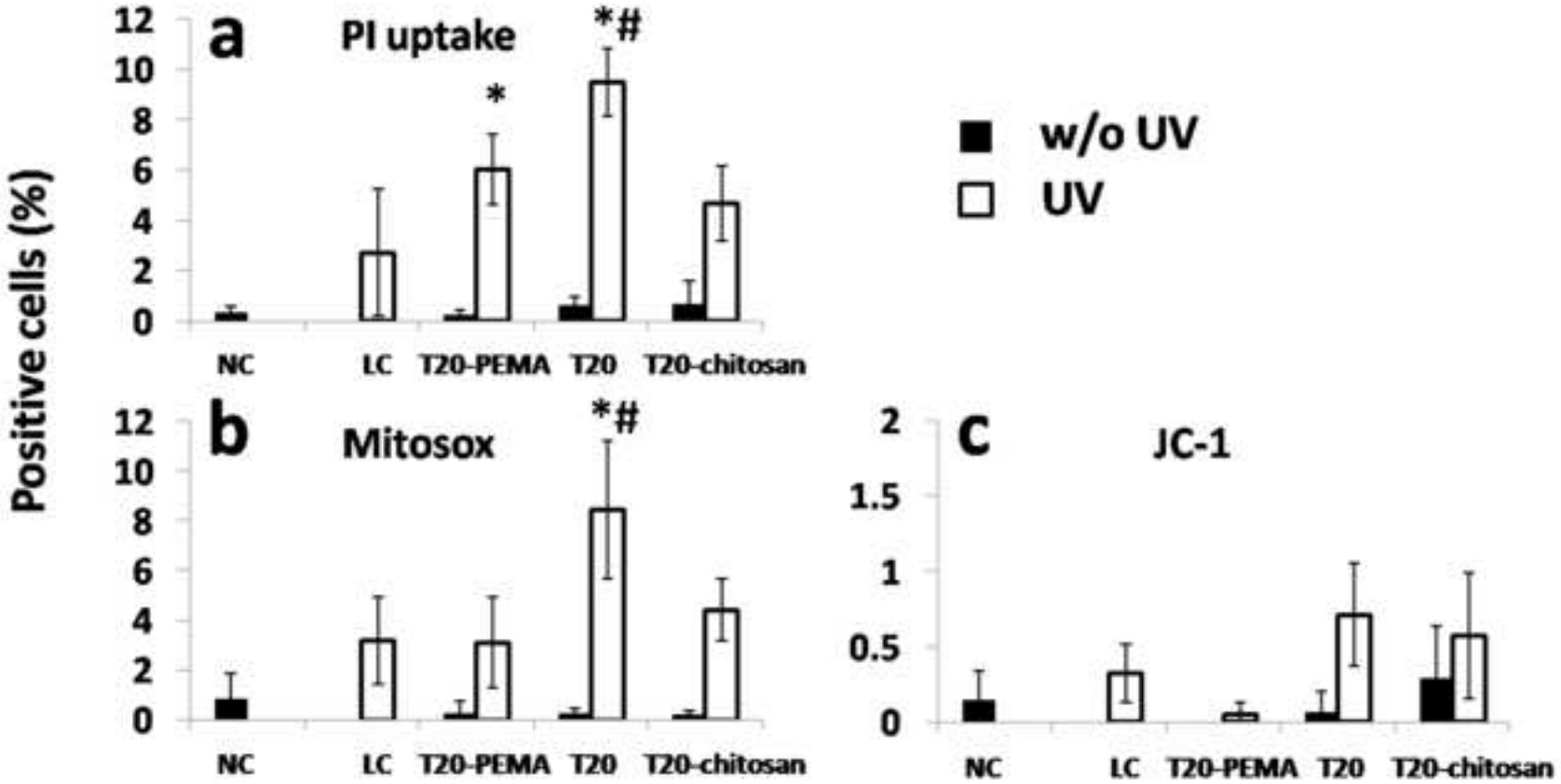
a
PI uptake
*
*#
b
Mitosox
*#
c
JC-1
Positive cells (%)
w/o UV
UV
NC
LC
T20-PEMA
T20
T20-chitosan

Figure 5

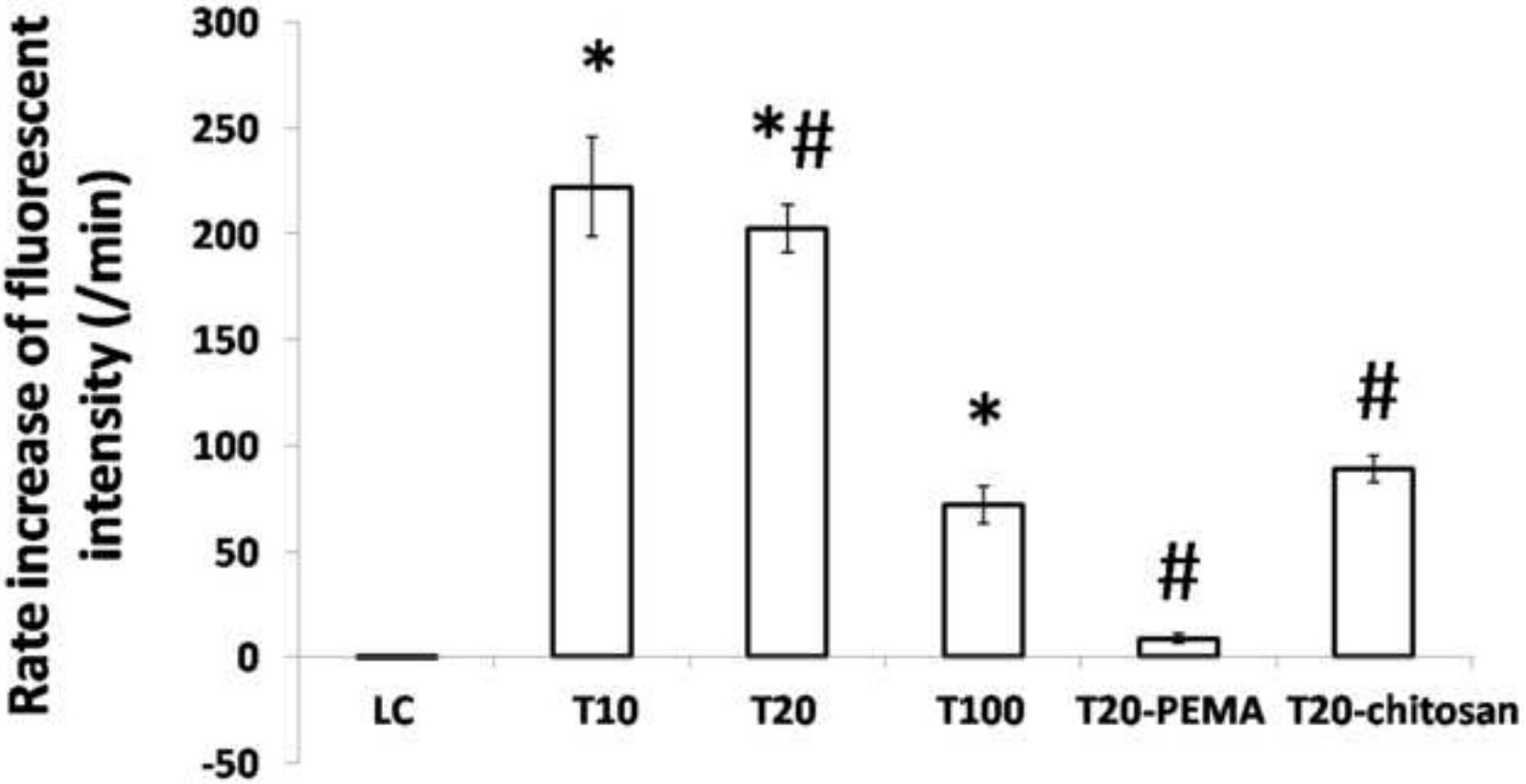
Rate increase of fluorescent intensity (/min)
300
250
200
150
100
50
0
-50
*
*#
*
#
#
LC
T10
T20
T100
T20-PEMA
T20-chitosan

Figure 6

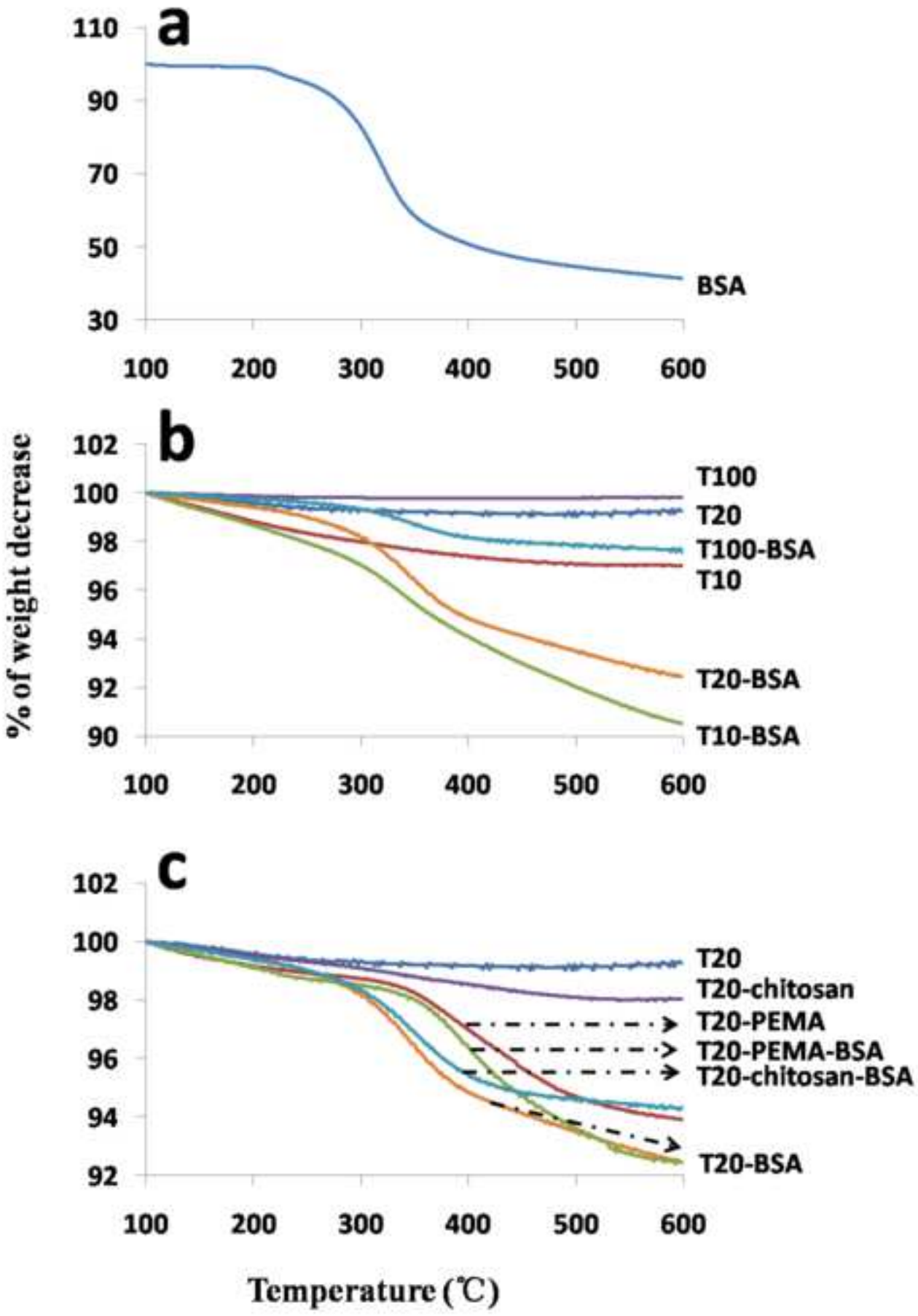
a
110
90
70
50
30
BSA
100
200
300
400
500
600
b
102
100
98
96
94
92
90
T100
T20
T100-BSA
T10
T20-BSA
T10-BSA
% of weight decrease
c
102
100
98
96
94
92
T20
T20-chitosan
T20-PEMA
T20-PEMA-BSA
T20-chitosan-BSA
T20-BSA
Temperature (℃)

Figure 7

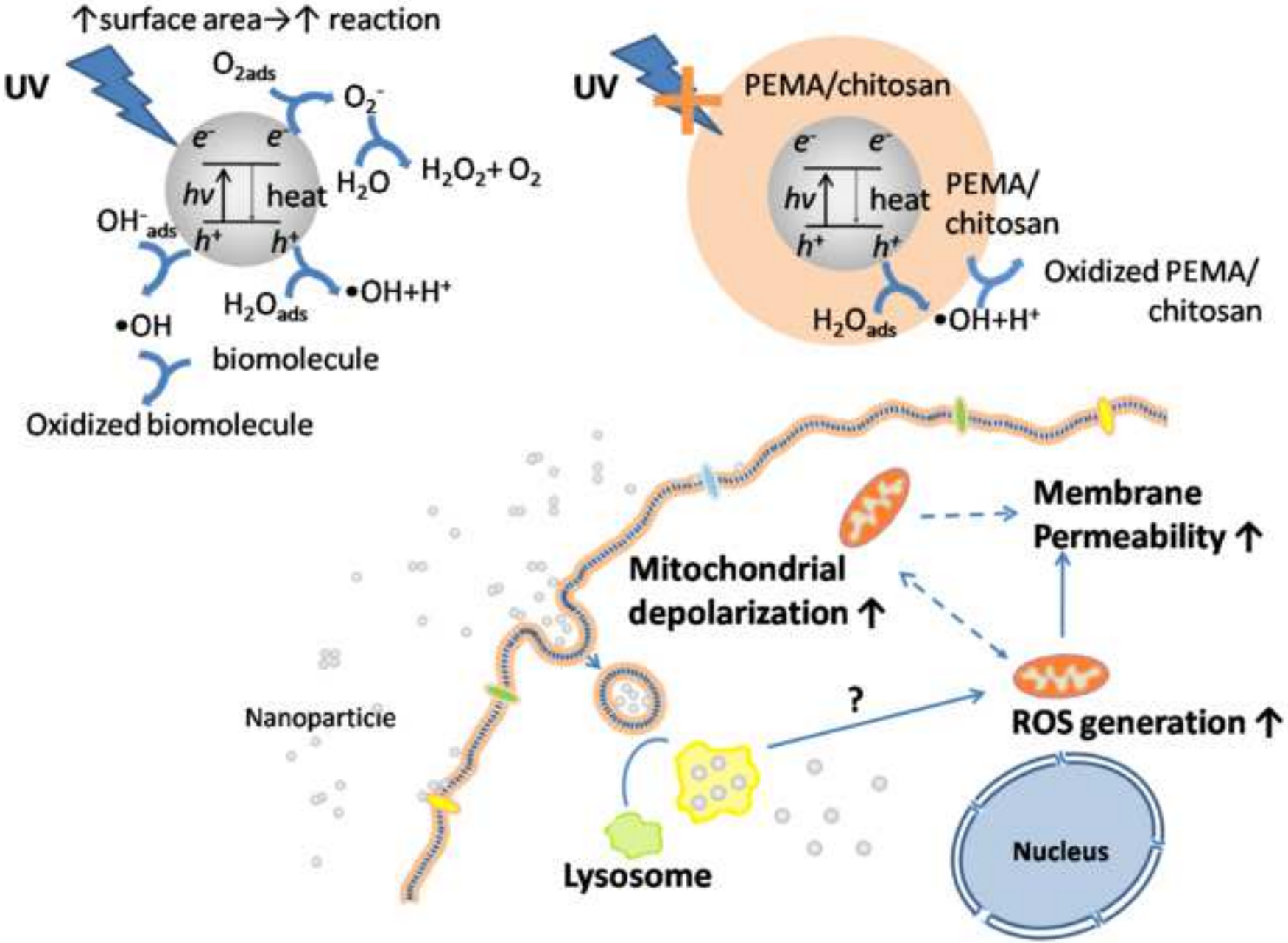
↑surface area→↑ reaction
UV
O_{2ads}
O_2^-
e^- e^-
hv
heat
h^+ h^+
H_2O
$H_2O_2+O_2$
OH^-_{ads}
H_2O_{ads}
•OH+H⁺
•OH
biomolecule
Oxidized biomolecule
UV
PEMA/chitosan
PEMA/
chitosan
Oxidized PEMA/
chitosan
Membrane
Permeability ↑
Mitochondrial
depolarization ↑
Nanoparticle
?
ROS generation ↑
Lysosome
Nucleus